IEEE Access
Multidisciplinary | Rapid Review | Open Access Journal

Received November 21, 2017, accepted December 22, 2017, date of publication January 9, 2018,
date of current version February 28, 2018.

*Digital Object Identifier 10.1109/ACCESS.2018.2791099*

# Correction of Wavefront Tilt Caused by Atmospheric Turbulence Using Quadrant Detectors for Enabling Fast Free-Space Quantum Communications in Daylight

**VERONICA FERNANDEZ[1], JORGE GÓMEZ-GARCÍA[1], ALEJANDRO OCAMPOS-GUILLÉN[1], AND ALBERTO CARRASCO-CASADO[2]**

[1]Spanish National Research Council, Institute of Physical and Information Technologies (CSIC), 28006 Madrid, Spain
[2]Space Communications Laboratory, National Institute of Information and Communications Technology (NICT), Koganei 184-8795, Japan

Corresponding author: Veronica Fernandez (veronica.fernandez@iec.csic.es)

This work was supported in part by the Ministerio de Economía y Competitividad, under Grant TEC2015-70406-R (MINECO/FEDER, UE), in part by the Fondo Social Europeo through Pograma Operativo de Empleo Juvenil, and in part by the Youth Employment Initiative through the Consejería de Educación, Juventud y Deporte of the Community of Madrid.

**ABSTRACT** Low photon-level signals used in most free-space quantum communication systems require a narrow field of view in the receiver to minimize the amount of background noise coupled into the single photon detectors. This can be achieved through beam tracking techniques, which compensate atmospheric effects, such as beam wander, in the receiver, reducing the long-term beam area. However, reducing the diameter of this area below a few microns, typically necessary to achieve a low level of solar background noise and successful daylight quantum transmission, require fine tracking precision and diffraction-limited optics. We demonstrate that this can be done with standard voice-coil fast steering mirrors and cheap commercially-available quadrant detectors. Two correcting strategies (open and closed loop) are experimentally tested and analyzed for their applicability in metropolitan (∼km range) free-space quantum communications. The area containing the random fluctuations of the beam centroid caused by atmospheric turbulence at the focal plane of the receiver was reduced by a factor of 4 with an open-loop configuration, and up to a factor of nine with a closed loop configuration. This is equivalent to a reduction in the quantum bit error rate caused by background solar noise of up to one order of magnitude, which, combined with spectral filtering techniques, enable the possibility of fast daylight quantum key distribution.

**INDEX TERMS** Beam steering, free-space quantum communication, quantum cryptography, wavefront tilt correction.

## I. INTRODUCTION

Quantum Key Distribution (QKD) [1] enables the information-theoretical secure distribution of cryptographic keys among two or more users. Practical implementations have reached distances of 250 km and beyond in fiber-based links [2]; 144 km in terrestrial free-space links [3]; and recently the first quantum-limited transmissions from space to ground have been demonstrated [4], [5]. Aside from these long range demonstrations, shorter (∼km range), high-speed, free-space optical (FSO) links are also useful in a variety of scenarios, such as for providing higher bandwidths in points of the metropolitan fiber-optic networks affected by dense data traffic, connecting points with difficult accessibility, or in cases where quick re-establishment of communications is necessary (such as in the event of natural catastrophes). FSO links can be laid easily, quickly and can connect efficiently these points with poor connectivity. They also offer portability, which is a valuable quality in the constantly changing and evolving communication market. If these free-space links also include a quantum communication channel, special care must be paid to filter out background photons from the sun or other artificial light sources since otherwise increase the error of these systems. This cannot be counteracted by increasing the signal power, already set to low — typically single-photon level — and quantum amplification is not yet possible with current technology.

It should be mentioned that for other QKD systems, such as those based on continuous variables, background noise is not a problem, since homodyne detection is immune to stray light. In discrete-variable systems though, it is a very limiting factor. Spectral, spatial and software filtering techniques are usually employed to decrease the amount of background noise, although they are usually not sufficient, and daylight performance is affected by limited key transmission rates [6]–[10].

Reducing the field of view of the receiver's detectors is an obvious technique to decrease the amount of background noise coupled in the system. However, turbulence in the atmosphere induces wavefront distortions, such as beam wander, which causes random fluctuations of the beam at the receiver, and thus, increased losses in the system if the field of view is reduced below a certain limit. Fortunately, these losses can be reduced if active beam correction/tracking techniques are employed, although adaptive optics techniques are needed to further decrease these losses, especially when using small detecting areas or coupling into a single mode fiber (SMF) [11]. Beam tracking techniques can correct for the tip and tilt errors of the wavefront (induced by atmospheric turbulence and jitter from building vibrations), stabilizing the beam centroid in the receiver plane. This plane in quantum communications is usually the focal plane where the long-term beam diameter is already reduced to tens of microns, typically, and the signal to noise ratio is low, which makes correction difficult. It should be stressed that only compensating in the receiver is sufficient when the beam deviations in the receiver caused by turbulence are smaller than the receiver aperture. This depends on the source's wavelength, the size of both the transmitter and receiver's apertures and the turbulent regime [12]. In particular, for the QKD system developed by this group [10] with transmitter and receiver's apertures of 4 cm and 8 cm, respectively, compensation in the receiver alone is enough to mitigate beam wander effects up to distances of 800 m under strong turbulent regimes ($C_n^2 \sim 10^{-13}$ m$^{-2/3}$) and 1.7 km and 2.5 km for $C_n^2 \sim 10^{-14}$ m$^{-2/3}$ and $C_n^2 \sim 10^{-15}$ m$^{-2/3}$, respectively. For longer distances or higher turbulent regimes precompensation in the transmitter is also needed. The impact of turbulence and its compensation is relatively unexplored in quantum communications with few studies on the field [13]–[16], although it has great potential for improving the Quantum Bit Error Rate (QBER) and enabling higher key rates [11], [12], which is an essential demand for quantum communications becoming widely implemented. Some studies have been aimed to maintain the link efficiency in the presence of slowly varying turbulence [3], [17]. In this paper, we will present a system for correcting beam wander effects in the presence of fast-varying turbulence using cheap and off-the-shelf quadrant position sensitive detectors (QDs), for its application in free-space quantum communication systems. The paper is organized as follows: section II gives a brief theoretical introduction of the effects of atmospheric turbulence in free-space optical links; section III discusses the performance of the position-sensitive detector technology in beam tracking systems; sections IV and V discuss two different correcting strategies for atmospheric turbulent effects: open and closed-loop; and section VI offers an estimation of the performance of the correcting strategy at longer distances.

## II. EFFECT OF ATMOSPHERIC TURBULENCE ON OPTICAL LINKS

The presence of gradients in the air density throughout the transmission channel causes wavefront distortions, which includes beam broadening, beam wander and scintillation. Beam broadening causes an enlarged beam, usually referred to as the *short-term* beam, (of radius $w_{st}$). The value of this radius can be predicted and accounted for by a suitable selection of the transmitter and receiver apertures, since an optimal value for both can be calculated as a function of the turbulent regime and the link length [12], [18]. The movement of the instantaneous center of the short-term beam at the receiver is usually called *beam wander* [19] and induces fluctuations in the *angle-of-arrival* (AOA), represented by $\beta_a$, i.e., in the direction of the incoming beam at the receiver (considered simply as a convergent lens of focal length $f$ in Figure 1). $\beta_a$ can be expressed as the *root-mean-square* (rms):

$$\sqrt{\langle \beta_a^2 \rangle} = \sqrt{2.91 C_n^2 L \, (2w_G)^{-1/3}} \tag{1}$$

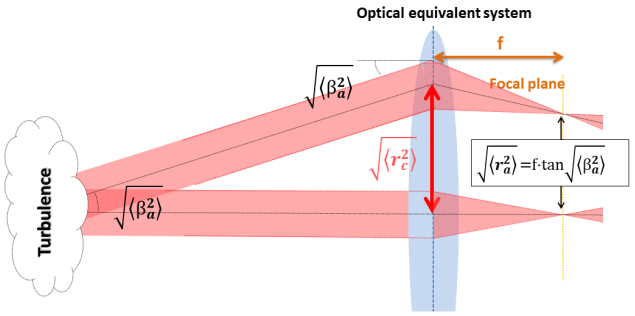


**FIGURE 1.** Rms displacement of the focal point or spot focal wander, $\sqrt{\langle r_a^2 \rangle}$, originated by fluctuations of the angle of arrival, $\sqrt{\langle \beta_a^2 \rangle}$.

where $C_n^2$ is the refractive index structure parameter, $L$ is the length of the link, and $w_G$ is the radius of the receiver aperture. These fluctuations in the angle of arrival result in spatial displacements of the instantaneous position of the beam centroid at any plane of the receiver. They appear as a random 'dancing' of the spot, which at the focal plane of the receiver are sometimes referred to as *focal spot wander*, which can be expressed as:

$$\sqrt{\langle r_a^2 \rangle} = f_{eff} \cdot tan \sqrt{\langle \beta_a^2 \rangle} \tag{2}$$

where $f_{\text{eff}}$ is the effective focal length of the receiver system. It is considered that the most important source of error of atmospheric turbulence is caused by the beam wander effect [20] and thus, the most substantial error reduction takes place through the correction of the angle of arrival or

*tilt*, which is the effect of beam wander [21]. The Field of View (FOV) is reduced by decreasing $\langle r_a^2 \rangle^{1/2}$ since this allows decreasing the detector aperture of the receiver, which in our case is the optical fiber at the focal plane that guides the received quantum signal to the single-photon detectors.

When treating atmospheric turbulence as a statistical process, the long-term beam radius $w_{LT}$ is a very useful modeling magnitude, since it gives account of the resulting effect of all the turbulence-related phenomena at the end of the propagation path. Beam wander can be statistically characterized by the variance of the displacement of the short-term beam centroid from the optical axis $\langle r_c^2 \rangle$. The long-term beam is the result of eddies of all sizes. In particular, eddies larger than the beam diameter produce the refractive effect related to beam wander. The short-term beam is originated by eddies that are smaller than the beam size, causing a broadening of the beam. The relationship between the long-term beam radius $w_{LT}$, the short-term beam radius $w_{ST}$ and the beam wander variance $\langle r_c^2 \rangle$ for a Gaussian beam is described by [19, eq. 3]:

$$w_{LT}^2 = w_{ST}^2 + \langle r_c^2 \rangle \tag{3}$$

The variance $\langle r_c^2 \rangle$ can be defined by equation (4), as a function of the refractive index structure parameter $C_n^2$, the link length $L$, and the transmitted beam radius $w_0$:

$$\langle r_c^2 \rangle = 2.42 \cdot C_n^2 \cdot L^3 \cdot w_0^{-1/3} \tag{4}$$

The long-term beam radius $w_{LT}$ can be described by equation (5), valid for Gaussian beams and all turbulent regimes [19]:

$$w_{LT} = w_Z \sqrt{1 + 1.63 \sigma_R^{12/5} \cdot \frac{\Lambda_0}{1 + \Lambda_0^2}} \tag{5}$$

where $w_Z$ is the beam radius at any distance $z$ of the optical axis, $\sigma_R^2$ and $\Lambda_0$ are the Rytov variance and the propagation parameter, respectively, defined by:

$$\sigma_R^2 = 1.23 \cdot C_n^2 \cdot k^{\frac{7}{6}} \cdot L^{\frac{11}{6}}; \qquad \Lambda_0 = \frac{2L}{k w_0^2} \tag{6}$$

and $k$ is the wavenumber. Scintillation is caused by constructive and destructive interference of the wavefront, which can lead to signal fading and considerably degrade their performance [22]. Although experimental work has shown that the effects of scintillation do not seem to significantly affect quantum key distribution systems [23], recent simulations for satellite quantum communications [11] show it should be considered in certain cases, especially when coupling into single mode fiber in strong turbulent regimes. Nevertheless, the correcting system in this study was designed to compensate only for wavefront tilt, in order to evaluate how this correction alone improves the performance of short-distance QKD systems.

## III. CORRECTING BEAM WANDER EFFECTS WITH POSITION SENSITIVE DETECTORS

The simplest configuration for optical beam stabilizing usually involves an actuator for controlling the optical beam, such as a Fast Steering Mirror (FSM), driven by a Proportional Integrative Derivative (PID) control, which is fed by the data provided by a Position Sensitive Detector (PSD). The PID control minimizes the error between a predetermined position signal of the PSD and the signal given by PSD in the presence of the atmospheric turbulence to be corrected.

There are two main technologies of PSDs: Segmented or Quadrant detectors (QDs) and Non-segmented or Lateral-Effect detectors (LEs). QDs have four or more active areas (see Figure 2) separated by an insensitive area known as *gap*, whereas LEs have a single active area. In both cases, the positions over the horizontal and vertical axes $x$ and $y$ are calculated as:

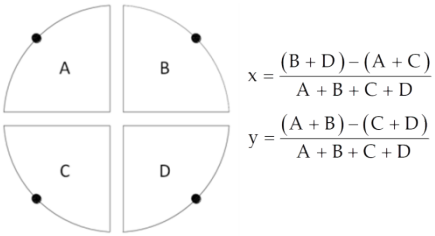


**FIGURE 2.** Diagram of a quadrant detector (left) and the equation for finding the position of the spot, x and y, (right) from the currents received in the terminals A, B, C, and D.

where A, B, C and D represent the current measured at each terminal of the device.

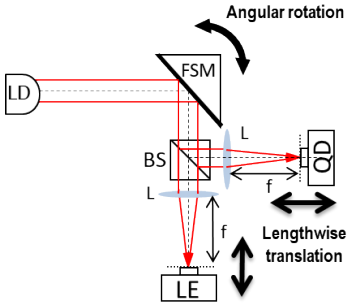


**FIGURE 3.** Optical setup for the characterization of the QDs and the LEs. LD is a laser diode; FSM is a fast steering mirror; L is a lens with 30 mm focal distance, f; QD is a quadrant detector and LE is a lateral effect detector.

In order to characterize the response of both detectors, the simple setup of Figure 3 was used. After proving that wavelength dependency of beam wander is negligible for our spectral range (850-1550nm) [24], a visible wavelength (of 670 nm) was used for the source for simplicity purposes. A 11mm-diameter collimated beam was directed to a voice-coil FSM (angle resolution of 0.4 $\mu$rad and a measured

bandwidth 3 dB of 500 Hz[1]), which was programmed to provide a *constant* angular sinusoidal deflection to the beam. This beam was then divided by a 50/50 beamsplitter into two paths where a QD and LE detectors were mounted on each arm on precision platforms. The selected QD was a IGA-030-QD from EOS Systems, with a 3 mm-diameter sensitive area, rising time of 25 ns (bandwidth equals to BW=0,35/25ns=14MHz) and a 46-$\mu$m gap. The LE detector was a C10443-02 from Hamamatsu, with a square geometry of 9×9 mm and a 16-KHz bandwidth. It is known that QDs have generally an associated higher spatial resolution (sub-micron) and LEs higher spatial range since they are not limited by the gap.

Two achromatic doublets with a focal length of 30 mm focused each beam to an approximate diameter of 40 $\mu$m at the focal plane. Each detector was then translated axially around the focal point (from a few millimeters before the focal point to a few millimeters after it). The experimental measured output signals of the QD and LE are shown on Fig. 4.

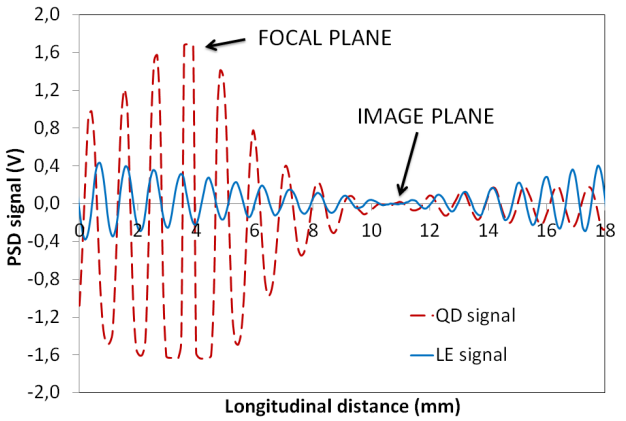


**FIGURE 4.** Experimental output response of a lateral-effect (continuous line) and quadrant (dashed line) detectors, for an angularly rotating beam hitting their surface as they are translated along the optical axis.

From Figure 4 it can be observed that the amplitude of the movements that the LE detects decreases as the detector is moved towards the focal of the lens. When the output amplitude of the movements becomes null, the image plane of the FSM is found. The focal point will be located at some distance before this image plane but cannot be easily found from the output trace. Conversely, the focal plane of the QD is found for the maximum amplitude of the detector's output.

This behavior can be understood by looking at Figure 5, which shows the (simulated) output response of the IGA-030-QD detector for beams of different sizes moving from one side of the detector to the opposite in the horizontal axis, $x$. The response is characterized by a saturated region where the output voltage, $V$ is constant and corresponds to the instances where the beam only hits two of the

[1]This bandwidth was reduced down to ∼200 Hz, to reject higher frequency atmospheric components.

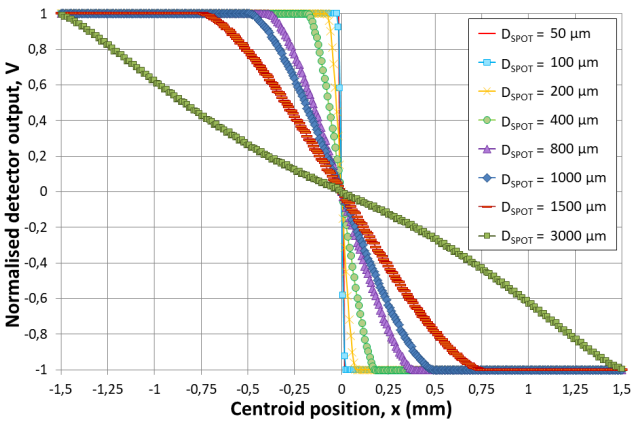


**FIGURE 5.** Normalized output voltage, $V$, of detector IGA-030-QD for different spot diameters $D_{spot}$, as a function of the centroid horizontal position, $x$.

four quadrants. This can be seen from equation in Figure 2. If the currents $A$ and $C$ are zero, $x$ takes a maximum value. When all four quadrants are being hit the output of the detector varies with the centroid position, $x$, and the detector enters the *linear region.* The smaller the beam spot is, the smaller this linear region is (since the region where the spot hits the four quadrants is smaller), and the larger the output response becomes. A compromise thus exists between the size of the detecting region and the detector's sensitivity. This means that in the focal plane the QD is very sensitive but its linear region is smaller.

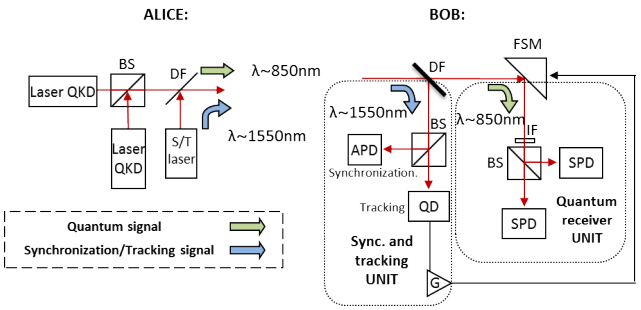


**FIGURE 6.** Compensation in the receiver for a two-state QKD system in an open-loop configuration. BS is a beamsplitter; DF is dichroic filter; APD is an avalanche photodiode; FSM is a fast steering mirror; IF is an interference filter; QD is a quadrant detector; SPD is a single-photon detector and G is the gain of a proportional integrative derivative control.

## IV. OPEN-LOOP CORRECTING STRATEGY

The turbulence compensation system in this work was designed for a QKD system described in [10] which uses a wavelength of 850 nm for the quantum signal and 1550 nm for the synchronization signal. Both signals travel through the same optical path in the transmission channel and undergo the same atmospheric disturbances. Having proved that beam wander affects them both similarly [15], [24] a possible design involves using part of the synchronization signal in the receiver for performing the turbulence compensation (see Figure 6), simplifying the design. However, other options

are also possible, such as using an additional laser in the emitter to perform the tracking in the receiver. Despite introducing a new laser in the emitter and possibly, an extra dichroic filter in the receiver for spectral discrimination; it can facilitate the alignment when a visible wavelength is used.

The simplest tracking configuration in the receiver consists of an open-loop between the detected centroid position given by a QD and the control signal generated by a PID control to a FSM. Figure 6 shows an open-loop tracking configuration for a two-state QKD system. In open-loop configuration, the correction is applied 'blindly' in the tracking channel, i.e., the correction is not observed here, but only in the quantum channel.

A simplified version of the setup shown in Fig. 6 was used for characterizing the performance of an open-loop configuration using the QD in the tracking channel (see Fig. 7). In our case, we used a red ($\lambda \sim 670$ nm) laser to perform the tracking since the wavelength did not affect qualitatively the correction and assessing the best strategy/detector was the priority. A collimated 11-mm diameter beam, mounted on a precision gimbal platform, was launched through open windows from emitter to receiver, located at a different laboratory at ITEFI-CSIC, and separated by 35 m of air.

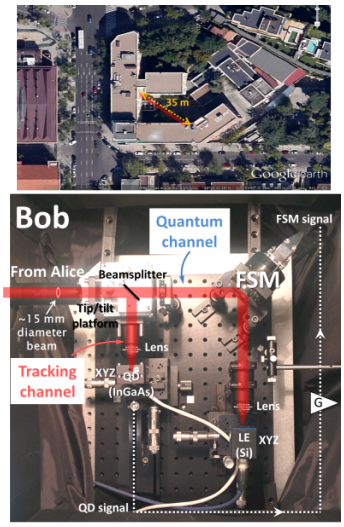


**FIGURE 7. Top: photograph showing a satellite view of the link between the emitter and the correcting receiver. Bottom: Experimental setup of the correcting receiver in an open-loop configuration. BS is a beamsplitter; FSM is a fast steering mirror; QD and LE are quadrant and lateral-effect position sensitive detectors, respectively; G is a proportional-integral-derivative loop control and XYZ are three-axis micro-positioner stages.**

The basic operation of this configuration consists in feeding the FSM with the position signal of the QD. The FSM is calibrated to generate a signal of different sign to that detected by the QD and whose gain is adjusted until the deviations observed in the LE are minimized. Both detectors (QD and LE) do not need to be placed at equivalent planes, as long as the generated signals by both have a constant relation between them, since this difference is compensated by adjusting the gain. However, this relation is constant as long as the QD response is linear. Therefore it is important to place the QD in a plane where the linear region is large, i.e., far from the focal plane. A LE, on the other hand, is placed at the focal plane in the quantum channel to monitor the correction performed by the FSM. The LE is placed where the single-photon detectors will be in the final QKD system, i.e., at the minimum field of view of the receiver.

In this type of configuration, the correction performed by the FSM only affects the quantum channel and not the synchronization channel. This means the synchronization beam is not corrected and signal losses can occur. However, since no power restrictions are imposed on this signal, as it is the case for the quantum signal, this can be taken into account by ensuring that the detector's field of view in the synchronization channel is sufficiently large to accommodate the turbulent fluctuations, such as selecting a sufficiently large collecting fiber for this channel.

Figure 7 shows the setup used for characterizing the correction by this strategy for the 35 m link. The emitter sent a ~11 mm diameter red beam which reached ~15 mm at the receiver's lens prior to the detectors (of 30 mm focal length). The results are shown in figure 8, where a histogram indicates how much the beam deviates from its predetermined optimum (zero) position, i.e., how many samples are measured as a function of the distance to the optimum position for a time interval of 30 seconds. This analysis provides a measure of the frequency of the deviations by the beam spot from its center. Enclosed in this figure there is a capture of the beam centroid position detected by the LE at the focal plane when the feedback loop of the correction system is deactivated (left) and activated (right) for real turbulence in the 35 m link. Considering a circle of events with ratio equal of the standard deviation, its ratio varies from 3.94 $\mu$m without correcting to 1,98 $\mu$m with correction, which is a factor of 2 times a lower ratio and 4 times a lower area. This reduction is equal to the reduction in QBER caused by solar background photons, since this can be expressed as:

$$QBER_{background} = \frac{B_{bckg}}{2B_{sifted}} \tag{7}$$

where $B_{bckg}$ is the rate of photons that reach the receiver's detectors due to solar background and $B_{sifted}$ is the sifted photon rate at Bob (usually much larger than $B_{bckg}$). When the focal spot area is reduced, $B_{bckg}$ is reduced in the same amount (assuming a collecting aperture with diameter equal to that of the corrected beam diameter is used in the receiver) whereas $B_{sifted}$ is practically constant since the vast majority of these photons come from the quantum signal (i.e., we can depreciate the photons from solar background noise from the photons coming from the quantum signal). Therefore a factor of 4 (or a 75%) decrease in the focal spot area is equivalent to the same decrease in $QBER_{background}$.

The main advantage of this strategy is that the correction planes at the tracking and quantum channels do not necessarily need to be the same. This means that the QD

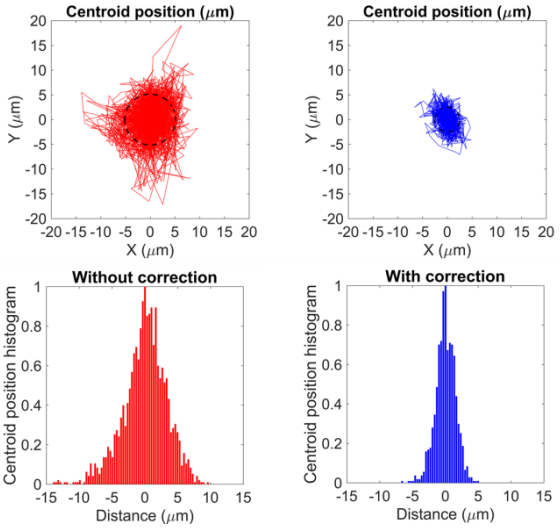


**FIGURE 8.** Top: beam centroid position at the focal plane without and with correction (the ratio of the dashed line circle shows the standard deviation). Bottom: Histogram of the beam centroid position at the focal plane of the quantum channel for an open-loop configuration with a quadrant detector in the tracking channel during a time interval of 30 seconds in a 35 m link. (Acquisition rate: 100 Hz).

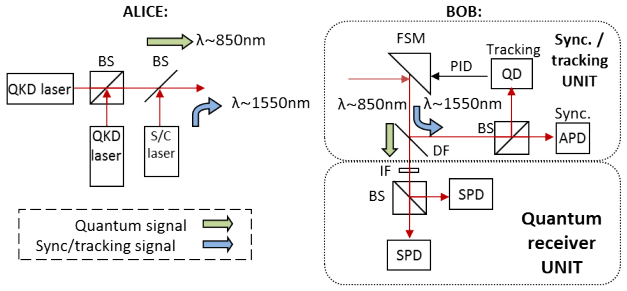


**FIGURE 9.** Compensation in the receiver for a two-state QKD system in a closed-loop configuration. BS is a beamsplitter, FSM is a fast steering mirror; DF is dichroic filter; APD is an avalanche photodiode; IF is an interference filter; QD is a position sensitive detector; PID is a proportional-integrative-derivative control; and SPD is a single-photon detector.

detector in the tracking channel performing the correction can be placed at any plane, i.e., so the focal plane can be avoided. This is an important advantage, as QD detectors should be preferably used with unfocused beams to increase the linear region and avoid the spot falling into the gap area, as discussed previously. The disadvantage of this type of configuration is the pre-calibration that must be performed in the presence of the real turbulence to be corrected. If the nature of this turbulence changes, for example if the system is calibrated to correct turbulence mainly originated near the transmitter, and this changes to a turbulence originated near the receiver the correction will not work efficiently and the system will have to be re-calibrated.

## V. CLOSED-LOOP CORRECTING STRATEGY

Having seen the limitations by the open-loop strategy, a more robust configuration for compensating AOA fluctuations in the receiver is the closed-loop correction strategy, since all deviations of the beam centroid can be corrected at a single plane, independently of their origin. Therefore no successive calibrations are needed if the turbulence changes its origin, aside from a first calibration to adjust the amplitudes of the QD detector and the FSM. This strategy allows real-time monitoring of the turbulence correction, since the FSM is placed before the quantum and tracking channels (see Figure 9).

In this strategy the detectors at the tracking and quantum channels must be placed at equivalents planes. It should be stressed that for these two planes to be equivalent not only they must be at the focal plane of the lenses, but the distance of each detector to the FSM must be equal [12]. In order to reduce the amount of solar background coupled into the receiver; this plane should be the focal plane, since the field of view is minimized in this plane. However, working in the focal plane implies that deviations of the beam are highly minimized and the signal to noise ratio (SNR) was very poor. Since the output of the LE is dependent on the SNR, its generated signal was of the same order as the electronic noise, and thus, not sufficient to achieve a good correction.

A QD was used instead, whose response is not dependent on the SNR and it is more sensitive to small beam deviations, such as those experienced at the focal plane, since its output voltage actually becomes maximum (see Figure 4). However, the spot reaches its minimum size in the focal plane which can cause problems due to the gap.

The closed-loop correcting strategy with a QD in the tracking channel was first tested at 35 m (the setup is basically that shown in figure 3, with a PID loop between the quadrant and the FSM and both detectors placed at the focal length distance of each lens). However, no correction was observed in the quantum channel. This was mainly due to aberrations on the spot profile, which combined with the spot being too small compared to the size of the gap (50 $\mu$m to 45 $\mu$m in diameter, respectively), made the correction by the quadrant impossible. The reason can be found from the operation of the QD, which 'finds' the spot center when the intensities are equilibrated in the four quadrants. When the spot has aberrations and a small size the majority of the intensity falls within the gap and therefore the QD has to center the remaining intensities, which sometimes causes the FSM to actually move the intensity centroid further away from the detector's surface. Therefore, $\langle r_a^2 \rangle^{1/2}$ is not zero after correction [25], as it should be in an ideal system. This value of $\langle r_a^2 \rangle^{1/2}$ can be considered as an error contribution due to aberrations that is impossible to correct by the FSM, since it is not caused by angular deflections of the beam. This contribution is generally caused by spherical aberration, since it has a dependence on the fourth power of $r$ (the distance from the center of the lens to the point where the beam hits the lens), and coma ($r^3$ dependence). Fortunately this problem can be minimized by a diffraction-limited optical

design for the receiver, which was achieved for a 100-meter link.[2] A Schmidt-Cassegrain telescope specially designed for minimizing spherical and coma aberrations and reducing the beam before the lenses to the detectors reduced aberrations below the diffraction limit.

The telescope focused a ∼45 mm-diameter received beam after 100 m of propagation path through air from Alice. A 250 mm-focal length $f_l$, was then used to collimate the beam and direct it to the tracking and quantum channels which was refocused in each channel by both 30mm-focal length $f_d$, lenses (see figure 10). A diffraction-limited spot of 7 $\mu$m in diameter was estimated through ray tracing software at the focal plane where the detectors were placed. This beam, free from aberration and in principle too small to be detected by the QD, was surprisingly large enough to provide correction. This is probably due to the Gaussian shape of the intensity profile and the high sensitivity of the QD in the focal plane. The standard deviation of the focal spot wander in the quantum channel was reduced in diameter up to a factor of 3 (depending on the turbulence intensity), which implies a reduction in area of up to 9 times (see figure 11). This is equivalent to a reduction in the QBER caused by background of ∼90%, which, according to our calculations would maintain a 1 Mbits/s secure key rate for the link demonstrated in [10] not only at nighttime, but also in daylight.

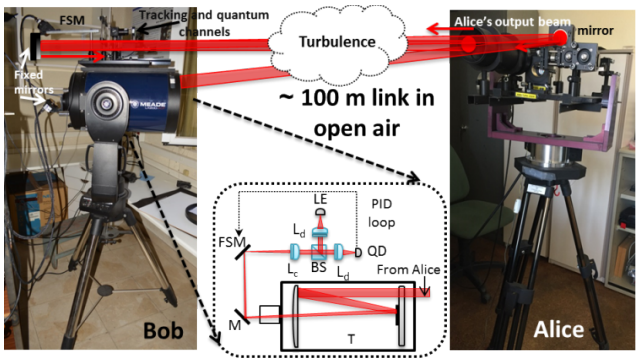


**FIGURE 10.** Picture of the receiver and sender of the closed-loop correcting system at 100 m. T is a Schmidt-Cassegrain 25 cm-diameter telescope, M is a fixed mirror; FSM is a fast steering mirror; Lc and $L_d$ are achromatic doublet lenses; BS is a 50/50 beamsplitter; LE and QD are lateral and quadrant position sensitive detectors; and PID is a proportional-integral-derivative loop.

The stability of the correction could also be verified by a 13-hour measurement where the *rms* value of the focal beam wander in the quantum channel was measured with and without correction as a function of the time of the day (Figure 12). It can be seen that the correction is maintained practically constant independently of the turbulence strength throughout the whole measurement. The reduction in $\text{QBER}_{\text{background}}$ estimated from the experimental values ranged from 61% to 90% for low and high values of the turbulence, respectively, with an average reduction value of 76%.

[2]This distance was obtained by reflecting the beam off two mirrors located at the receiver and emitter's rooms.

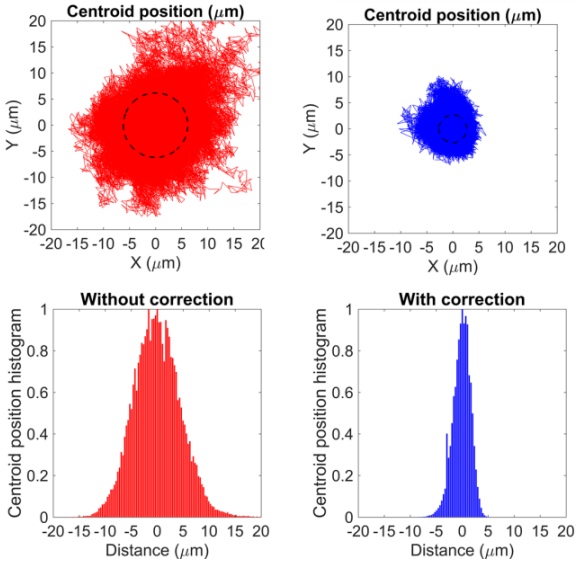


**FIGURE 11.** Top: beam centroid position at the focal plane without and with correction (the ratio of the dashed line circle shows the standard deviation). Bottom: Histogram of the beam centroid position at the focal plane of the quantum channel for a closed-loop configuration with a quadrant detector in the tracking channel during a time interval of 1 minute in a 100 m link. (Acquisition rate 2000 Hz).

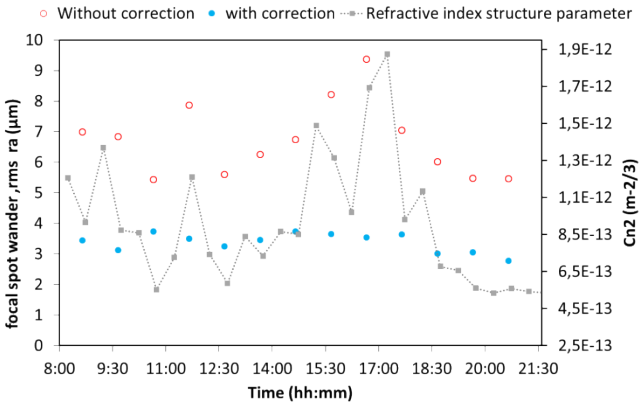


**FIGURE 12.** Root-mean-square of the focal beam wander and refractive index structure parameter $C_n^2$ without and with correction with 1FSM closed-loop correction for 100 meters over a time period of 13 hours.

## VI. ESTIMATION OF THE CORRECTION AT LONGER DISTANCES

In order to estimate the performance of the closed-loop correcting strategy shown in Figure 10 for longer distances than 100 m, the correction of the focal spot wander was simulated using ray tracing software. The value of the refractive index structure parameter $C_n^2$ to be used in the simulation was estimated by first estimating the angle of arrival $\langle \beta_a^2 \rangle^{1/2}$ from equation (2) and both the measured values of $\langle r_a^2 \rangle^{1/2}$ over time (Figure 12), and the effective focal length of the receiver (340 mm). With these values of $\langle \beta_a^2 \rangle^{1/2}$ and equation (1), $C_n^2$ can be calculated, which was found to range between ∼4, $5 \times 10^{-13}$ $\text{m}^{-2/3}$ and ∼$2 \times 10^{-12}$ $\text{m}^{-2/3}$ over

a time interval of 13 hours. These relatively high values of $C_n^2$ are due to the natural turbulence of the 100-m link being artificially increased with a strong flow of cool air from an air conditioning equipment in both the emitter and receiver's rooms, which was mixed with the warm air coming from the outside through the open windows whose temperature was ranging from 18 °C (at 8 am) to 29 °C (at 4 pm). On the other hand, the value of $\langle r_c^2 \rangle^{1/2}$ was calculated from equation (4) for each link length. In the simulation, the source was placed at the corresponding distance such that the rotation of $\langle \beta_a^2 \rangle^{1/2}$ generated the corresponding $\langle r_c^2 \rangle^{1/2}$. The maximum link length simulated was 800 m since this is the maximum distance where compensation in the receiver can be applied in the studied system without losing any quantum signal due to losses, in a strong turbulent regime ($C_n^2 \sim 10^{-13}$ m$^{-2/3}$) [12]. For longer distances, pre-compensation in the emitter must also be performed to avoid losses. The simulated and experimental values of the spot focal wander $\langle r_a^2 \rangle^{1/2}$ for 100 m were compared and found to be in good agreement (see Table 1). The shown values correspond to the highest measured $C_n^2$ of $1.7 \times 10^{12}$ m$^{2/3}$. The experimental values were taken over three consecutive intervals, each with one minute correction ON and one minute OFF, with a total duration of six minutes.

**TABLE 1. Simulated and experimental values of the rms focal spot wander ra and diameter of the receiver's collection aperture at the focal plane Df, before and after correction for a 100 m link.**

| | $\langle r_a^2 \rangle^{1/2}$ before correction (μm) | $\langle r_a^2 \rangle^{1/2}$ after correction (μm) | $D_f$ before correction (μm) | $D_f$ after correction (μm) |
|---|---|---|---|---|
| simulation | 8,6 | 3,5 | 23,3 | 12,7 |
| experiment | 9,4 ± 0,5 | 3,5 ± 0,5 | 20,5 ± 4,4 | 10,7 ± 0,6 |

An aperture of diameter $D_f$ at the receiver focal plane necessary to couple all the optical power was both estimated from the simulation and measured experimentally. This aperture defines the field of view, $\Delta\theta \approx D_f / f_{eff}$. It should be stressed that $D_f$ takes into account not only the deviations caused by atmospheric turbulence, but also the shape of the beam spot, which can be affected by aberrations. The experimental value of $D_f$ was obtained from equation (8), by measuring the optical power coupled into a SMF (single-mode fiber at $\lambda \sim 1550$ nm of radius a ≈5 $\mu$m), $P(a)$, placed at the focal plane of the receiver:

$$P(a) = P_{tot}\left(1 - e^{-\frac{2a^2}{w^2}}\right) \tag{8}$$

where $P_{tot}$ is the power measured before coupling into the optical fiber, $a$ is the radius of the fiber core, $w$ is the diameter of the beam at the focal plane, i.e., $D_f/2$. The experimental results were in good agreement with the simulation (see Table 1) and show an average reduction of $D_f$ (and therefore the FOV) after correction of a factor of two. The coupling efficiency $\eta_{coupling}$ $(P(a)/P_{tot})$ increased after correction from 0.35 to 0.8 (on average), which corresponds to a reduction in the $\text{QBER}_{(\text{background})}$ of 56%.

The simulation of the performance of the closed-loop correcting system for longer distances is shown in Figure 13 and $D_f$ is estimated for two types of lenses before the detectors $L_d$: firstly with $f_d = 30$ mm (the same we used in our setup) and secondly with a longer focal length $f_d$ of 50 mm. The reason for this is that up to a distance of 300 m, $D_f$ after correction is similar for either lens and therefore any of them can be used with similar results. However, for longer distances than 300 m, a longer focal lens reduces aberrations and improves the correction performed by the QD detectors. The expected reduction in $\text{QBER}_{(\text{background})}$ was calculated assuming that the receiver uses apertures equal to the values of the simulated $D_f$ before and after correction. A lens of $f_d = 30$ mm for distances up to 300 m and $f_d = 50$ mm for distances longer than 300 m are assumed.

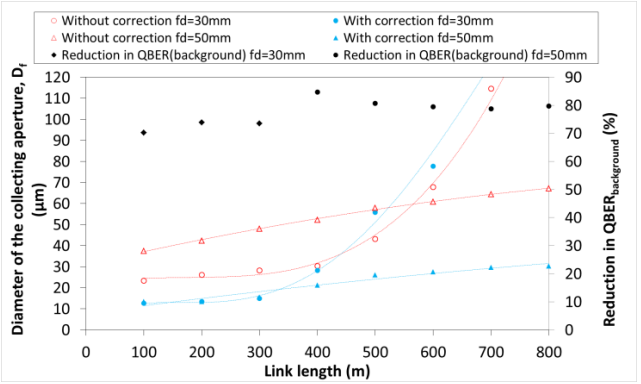


**FIGURE 13. Simulated diameter of the collection aperture, Df, with and without correction for a closed-loop correcting strategy as a function of the length of the link and for two types of lenses: a shorter and longer focal length. The reduction of $\text{QBER}_{(\text{background})}$ is also shown as a function of the link length.**

## VII. CONCLUSIONS

Free-space quantum communications aimed to complement metropolitan networks require fast and daylight operation, even under strong turbulent regimes, to satisfy the realistic bandwidth demands of the telecommunications industry. In this scenario, precise tracking of atmospheric beam fluctuations is essential to increase the SNR of the received quantum signal. Two tracking strategies were tested: open and closed loop. An open-loop configuration enabled a factor of 4 reduction in the area of long-term beam fluctuations in the focal plane of the receiver. However, this strategy needs of a recalibration when the turbulence changes its origin. On the other hand, a more robust closed-loop strategy corrects automatically all fluctuations independently of its origin and no recalibrations are needed. However, this strategy requires correcting in the focal plane of the receiver, whose area is limited to just a few microns in order to decrease the solar background noise coupled in the system. This imposes some challenges. Firstly, the low SNR in the focal plane

requires detectors with a non-SNR dependent response, such as QDs. Their high sensitivity at the focal plane allows efficient correction of atmospheric effects, despite the beam spot being smaller than the gap in this plane. This is due to the Gaussian shape of the beam, which allows the QD to sense subtle differences in intensities far from the Gaussian peak. However, since QD detectors equilibrate intensities instead of finding the beam centroid, they do not correct well when the beam spot has aberrations. Therefore it is crucial that the optics of the receiver generate diffraction-limited beam spots, which was achieved by using a Schmidt-Cassegrain telescope and adequate lenses. Taking into account all these factors a correction with the closed-loop strategy of up to 9 times a lower area at the focal plane of the receiver was obtained at 100 m, which implies a potential reduction of the QBER due to background of up to one order of magnitude. Simulations at longer distances predict a similar reduction at high turbulent regimes. This will enable considerable higher key rates in daylight even in the presence of strong turbulence, which are critical challenges in free-space QKD systems today.

## REFERENCES

[1] C. H. Bennett and G. Brassard, "Quantum cryptography: Public key distribution and coin tossing," in *Proc. IEEE Int. Conf. Comput., Syst. Signal Process.*, Bengaluru, India, Dec. 1984, pp. 175–179.

[2] D. Stucki *et al.*, "High rate, long-distance quantum key distribution over 250 km of ultra low loss fibres," *New J. Phys.*, vol. 11, no. 7, p. 075003, 2009.

[3] T. Schmitt-Manderbach *et al.*, "Experimental demonstration of free-space decoy-state quantum key distribution over 144 km," *Phys. Rev. Lett.*, vol. 98, no. 1, p. 010504, 2007.

[4] J. Yin *et al.*, "Satellite-based entanglement distribution over 1200 kilometers," *Science*, vol. 356, no. 6343, pp. 1140–1144, 2017.

[5] H. Takenaka, A. Carrasco-Casado, M. Fujiwara, M. Kitamura, M. Sasaki, and M. Toyoshima, "Satellite-to-ground quantum-limited communication using a 50-kg-class microsatellite," *Nature Photon.*, vol. 11, pp. 502–508, Jul. 2017.

[6] R. J. Hughes, J. E. Nordholt, D. Derkacs, and C. G. Peterson, "Practical free-space quantum key distribution over 10 km in daylight and at night," *New J. Phys.*, vol. 4, p. 43, Jul. 2002.

[7] J. L. Duligall, M. S. Godfrey, K. A. Harrison, W. J. Munro, and J. G. Rarity, "Low cost and compact quantum key distribution," *New J. Phys.*, vol. 8, p. 249, Oct. 2006.

[8] M. P. Peloso, I. Gerhardt, C. Ho, A. Lamas-Linares, and C. Kurtsiefer, "Daylight operation of a free space, entanglement-based quantum key distribution system," *New J. Phys.*, vol. 11, p. 045007, Apr. 2009.

[9] D. M. Benton, P. M. Gorman, P. R. Tapster, and D. M. Taylor, "A compact free space quantum key distribution system capable of daylight operation," *Opt. Commun.*, vol. 283, pp. 2465–2471, Jun. 2010.

[10] M. J. García-Martínez *et al.*, "High-speed free-space quantum key distribution system for urban daylight applications," *Appl. Opt.*, vol. 52, no. 14, pp. 3311–3317, 2013.

[11] M. T. Gruneisen, M. B. Flanagan, and B. A. Sickmiller, "Modeling satellite-Earth quantum channel downlinks with adaptive-optics coupling to single-mode fibers," *Proc. SPIE*, vol. 10442, p. 104420E, Oct. 2017.

[12] A. Carrasco-Casado, N. Denisenko, and V. Fernandez, "Correction of beam wander for a free-space quantum key distribution system operating in urban environment," *Opt. Eng.*, vol. 53, no. 8, p. 084112, 2014.

[13] I. Capraro *et al.*, "Impact of turbulence in long range quantum and classical communications," *Phys. Rev. Lett.*, vol. 109, p. 200502, Nov. 2012.

[14] G. Vallone *et al.*, "Adaptive real time selection for quantum key distribution in lossy and turbulent free-space channels," *Phys. Rev. A, Gen. Phys.*, vol. 91, p. 042320, Apr. 2015.

[15] F. Kullander, L. Sjöqvist, and P. Jonsson, "Effects of turbulence on a combined 1535-nm retro reflective and a low-intensity single-path 850-nm optical communication link," *Proc. SPIE*, vol. 6399, p. 639906, Oct. 2006.

[16] I. Capraro, "Advanced techniques in free space quantum communication," Ph.D. dissertation, Dept. Inf. Eng., Univ. Padova, Padua, Italy, Sep. 2008.

[17] H. Weier, T. Schmitt-Manderbach, N. Regner, C. Kurtsiefer, and H. Weinfurter, "Free space quantum key distribution: Towards a real life application," *Prog. Phys.*, vol. 54, nos. 8–10, pp. 840–845, Aug. 2006.

[18] A. Carrasco-Casado, "Contribuciones a las comunicaciones ópticas en espacio libre: Utilización de telescopios Cherenkov como receptores y corrección de Beam Wander en comunicaciones cuánticas," Ph.D. dissertation, Dept. Electron. Technol., Univ. Carlos III Madrid, Madrid, Spain, 2015.

[19] L. C. Andrews and R. L. Phillips, *Laser Beam Propagation Through Random Media*. Bellingham, WA, USA: SPIE, 2005.

[20] R. J. Noll, "Zernike polynomials and atmospheric turbulence," *J. Opt. Soc. Amer.*, vol. 66, no. 3, pp. 207–211, 1976.

[21] D. L. Fried, "Statistics of a geometric representation of wavefront distortion," *J. Opt. Soc. Amer. A, Opt. Image Sci.*, vol. 55, no. 11, pp. 1427–1431, 1965.

[22] I. I. Kim, M. Mitchell, and E. J. Korevaar, "Measurement of scintillation for free-space laser communication at 785 nm and 1550 nm," *Proc. SPIE*, vol. 3850, pp. 49–62, Sep. 1999.

[23] J. H. Shapiro, "Scintillation has minimal impact on far-field Bennett–Brassard 1984 protocol quantum key distribution," *Phys. Rev. Lett.*, vol. 84, p. 032340, Sep. 2011.

[24] A. Carrasco-Casado, N. Denisenko, and V. Fernandez, "Chromatic effects in beam wander correction for free-space quantum communications," *Microw. Opt. Technol. Lett.*, vol. 58, no. 6, pp. 1362–1365, 2016.

[25] J. Gómez-García, "Comparison of beam wander correction by quadrant and ideal detectors for aerial quantum communication links," M.S. thesis, Dept. Phys., Autonomous Univ. Barcelona, Barcelona, Spain, 2015. [Online]. Available: http://upcommons.upc.edu/handle/2117/80508

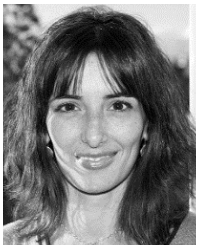

**VERONICA FERNANDEZ** received the B.Sc. degree (Hons.) in physics with electronics from the University of Seville in 2002, and the Ph.D. degree in physics from Heriot-Watt University, Edinburgh, U.K., in 2006, with title Gigahertz Clocked Point-to-Point and Multi-User Quantum Key Distribution Systems.

She joined the Institute for Physical and Information Technologies, Spanish National Research Council (CSIC), Madrid, in 2007, with a postdoctoral Juan de la Cierva contract. In 2009, she obtained a permanent position at CSIC. Her main research lines include experimental high-speed quantum key distribution systems, both in free space and optical fiber, and laser-beam stabilization systems for correcting atmospheric turbulent effects in optical and quantum communications.

**JORGE GÓMEZ-GARCÍA** received the degree in physics from the Complutense University of Madrid, in 2014, and the M.S. degree in photonics from the Polytechnic University of Catalonia in 2015.

Since 2016, he has been with the Department of Information and Communication Technologies, Institute of Physical and Information Technologies, Spanish National Research Council, Madrid. He is currently a Research Assistant, beneficiary of the Youth Employment Initiative and Operational Programme of Youth Employment, awarded by the Community of Madrid and the European Social Fund. He is currently investigating the correction of atmospheric effects for aerial quantum communication links.

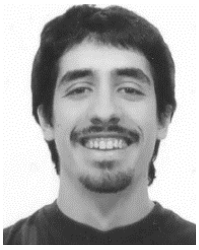

**ALEJANDRO OCAMPOS-GUILLÉN** received the degree in physics from the Autonomous University of Madrid in 2016, the M.S. degree in new technologies for electronics and photonics from the Complutense University of Madrid in 2017.

He completed his master's thesis with the Department of Information and Communication Technologies, ITEFI-CSIC, where he is currently a Research Assistant in 2017. He is a beneficiary of the Youth Employment Initiative and Operational Programme of Youth Employment, awarded by the European Social Found. His research interests focus on correction of atmospheric turbulent effects for quantum communication links.

**ALBERTO CARRASCO-CASADO** received the B.S. degree in telecommunication engineering from Málaga University, Spain, in 2005, the M.S. degrees in telecommunication engineering and the M.S. degree in space research from Alcalá University, Madrid, in 2008 and 2009, respectively, and the Ph.D. degree in electric, electronic, and automation engineering from the Carlos III University of Madrid and Spanish National Research Council in 2015. In 2015, he joined the Space Communications Laboratory, National Institute of Information and Communications Technology, Tokyo, Japan. His research interests focus on free-space optics, satellite communications, space engineering, and quantum cryptography.